Weierstraß-Institut
für Angewandte Analysis und Stochastik

im Forschungsverbund Berlin e.V.

Preprint ISSN 0946 – 8633

A milling model with thermal effects including the dynamics of machine and work piece

Oliver Rott[1], Patrick Rasper[2], Dietmar Hömberg[1], Eckart Uhlmann[2]

submitted: June 30, 2008

[1] Weierstrass Institute
for Applied Analysis
and Stochastics
Mohrenstraße 39
10117 Berlin
Germany
E-Mail: rott@wias-berlin.de
hoemberg@wias-berlin.de

[2] Technische Universität Berlin
Institut für Werkzeugmaschinen
und Fabrikbetrieb
Pascalstr. 8-9
10587 Berlin
Germany
E-Mail: rasper@iwf.tu-berlin.de
uhlmann@iwf.tu-berlin.de

No. 1338
Berlin 2008

2000 *Mathematics Subject Classification.* 74H99, 93A30.

Key words and phrases. Process machine interaction, stability, time domain simulation.

The financial support from Deutsche Forschungsgemeinschaft (DFG) within the priority program SPP 1180 "Prediction and manipulation of interaction between structure and process" is gratefully acknowledged.

Edited by
Weierstraß-Institut für Angewandte Analysis und Stochastik (WIAS)
Mohrenstraße 39
10117 Berlin
Germany

Fax: + 49 30 2044975
E-Mail: preprint@wias-berlin.de
World Wide Web: http://www.wias-berlin.de/

Abstract
This paper deals with the development of a new mathematical model that characterizes the structure-process interaction for a complex milling system. The structure is divided into a work piece and a machine part, which are represented by different models. While the machine dynamics is characterized by a standard multi-body system, the work piece is described as a linear thermo-elastic continuum. The coupling of both parts is carried out by an empirical process model permitting an estimate of heat and coupling forces occurring during milling.
This work reports the derivation of the governing equations emphasizing the coupling and summarizes the numerical algorithms being applied to solve the coupled equation system. The results of numerical simulations that show the dynamics of the complex thermo-mechanical system are presented at the end.

1 INTRODUCTION

The modeling of milling dynamics, the determination of stable cutting conditions and the design of more efficient milling machines are important research fields in production technology. Effective methods to predict stable processes have been developed in recent decades (cf. Altintas et al. [1], Faassen [2]). An essential part of these methods is an abstract dynamical model, i.e. an ordinary differential equation. Adjusted to vibration measurement data it reproduces local characteristics of the actual milling system, i.e. the dynamics at the tip of the cutter. In combination with a process model it allows to identify efficiently stable machining parameters by means of bifurcation analysis (cf. Faassen [3], Insperger [4], Szalai [5]).

However, these methods provide only few detailed information about the dynamics of the entire machine structure. To allow for more detailed studies we have developed a new mathematical model especially accounting for the process-structure interaction. The structural part of the model consists of two sub models. The first part is a multi body system representing the dynamical characteristics of the entire machine. Such a machine representation has the advantage that we may analyze the behavior of each structural component in detail. This information may be used to find out weak spots in the machine structure and provide hints to further improvements. The second part is a detailed work piece representation. The work piece is modeled as a continuous thermo-elastic body, incorporating the varying dynamics due to material removal. Thus, it allows for studying the effect of thermal expansion which may be important in the machining of thin walled pieces. The coupling of both sub-structures is carried out with an empirical cutting force model. The main part of the coupling is a new formulation of the uncut chip thickness which takes into account the work piece deformation. The forces arising in the milling process act on the work piece as well as on the cutter as member of the machine structure. In Section 2 we derive the model equations, describe a numerical algorithm and discuss the problem of parameter identification. We present some numerical results in Section 3. Section 4 is devoted to some concluding remarks.

2 MODELLING

2.1 The thermo elastic work piece model

We assume that the major part of the machined work piece behaves like thermo elastic solid. Only in vicinity of the cutting edge, which is a small domain compared to volume of the work piece, visco-elasto-plastic effects have to be taken into account. However, these effects will be incorporated through the empirical cutting force model (cf. Section 2.3). The corresponding equations can be found in the monograph Haupt [6]:

$$\begin{aligned} \rho_0 u_{tt} &= \nabla \cdot \sigma, \\ \sigma &= \lambda\left(\varepsilon : I\right) I + 2\mu\varepsilon - 3K\alpha\left(T - T_0\right), \\ \varepsilon &= \frac{1}{2}\left(\nabla u + \nabla^T u\right), \\ \rho_0 c_V T_t &= \kappa \nabla T - 3K\alpha T_0 \nabla \cdot v, \end{aligned} \tag{1}$$

where λ and μ are the Lamé constants, T_0 denotes a reference temperature, i.e. the initial temperature, κ the heat conductivity and α is the thermal expansion coefficient.

2.2 Machine model

Here, we assume that the milling machine can be represented by a rigid body system. The structural members of the machine (spindle, traverse, side-plates etc.) are coupled with linear spring-damper elements. A well known strategy to carry out the mathematical modeling of the rigid body system is to formulate the corresponding Newton–Euler–equations with additional constraints accounting for given system properties such as spindle rotation speed or feed displacements. This approach results in a system of differential and algebraic equations.

We follow an alternative strategy by formulating the Newton-Euler-equations in generalized coordinates. In this approach the number of generalized coordinates equals the number of degrees of freedom of the constrained system and we get no additional algebraic equations. In order to derive the equations of motion explicitly, we use an efficient technique, called the principal of Jourdain (cf. Pfeiffer [7]), which provides a compact expression for the Newton-Euler-equations of a N -body system given in generalized coordinates $q(t)$.

In order to model the kinematics of the multi body system, we draw up the position vectors to each center of mass, denoted in the global reference frame, using the generalized coordinates $q(t)$. The time derivative of the position vectors immediately yields the corresponding velocity and accelerations. We describe the orientation of the body fixed reference frames by applying orthogonal transformations on the global reference frame. The transformations consist of a product of rotation matrices based on Kardan-angles as described by Wittenburg [8]. These angles are also part of the generalized coordinates. It is easily seen that the angular velocities ω_i follow from the time derivates of the orthogonal transformations.

For the computation of the force F_i^e and torques M_i^e acting on body ‘i’, we have to describe the movement points ‘P’ on a rigid body as a function of the generalized coordinates. For this purpose we assume that the coordinates ${}^i r_P = ({}^i x_P, {}^i y_P, {}^i z_P)^T$ of a ‘P’ on the body ‘i’ are given in the reference frame attached to the body. In order to compute the position of point ‘P’ in the global reference frame ‘R’ we use the position vector ${}^R r_{S_i}$ and orientation of body ‘i’ relatively to the system ‘R’ in the following form:

$$ {}^R h_P(t,q) = {}^R r_{S_i}(t,q) + {}^R O_i(t,q)\, {}^i r_P. \tag{2} $$

Starting from this expression we may derive a formula for the relative displacement and the relative velocity of two points on two different bodies, which are necessary to compute the forces and torques acting via the coupling elements on each body.

The general equation of motion for the multi body system in generalized coordinates reads:

$$ M(q,t)\ddot{q} = f(\dot{q},q,t,p), \tag{3} $$

where p denotes the vector of stiffness and damping constants of the coupling elements.

2.3 Coupling

The basis for the coupling of work piece and machine model is the cutting force. To this end we use an algebraic relation for the uncut chip thickness and the cutting forces (cf. Weck [9]):

$$ \hat{F} = K \max(h,0). \tag{4} $$

On the cutting edge the forces act in three directions: perpendicular to the cutting velocity, in opposite direction to the cutting velocity and parallel to the rotation axis of the cutter. In order to obtain a general expression usable on the right hand side of equation (3) and to define a stress vector on the boundary of the work piece, we transform equation (4) into the global reference frame:

$$ {}^R f = g\left(\varphi_j(t,z)\right) {}^R O_C(t,q)\, {}^C A_F(\alpha_j, z)\hat{F}, \tag{5} $$

where $g = 1$, if the corresponding tooth 'j' with angle $\varphi_j(t,z)$ is in cut and $g = 0$ otherwise. The orthogonal matrix ${}^{C}A_{F}$ transforms the forces $\hat{F}$ into the reference frame attached to the cutter. The rotation matrix ${}^{R}O_{C}$ transforms the force vector into the global reference frame. Note that ${}^{R}f$ in equation (5), has the dimension force per length. Now we define the boundary condition for the momentum balance (cf. (1)) as:

$$u = 0 \quad on \quad \Gamma_D,$$
$$-\sigma \cdot n = \begin{cases} -\dfrac{{}^{R}f}{s_{\Gamma_F}}, & if \quad \vec{x} \in \Gamma_F(t), \\ 0, & otherwise. \end{cases} \tag{6}$$

The value s_{Γ_F} denotes the length of the arc where the stress vector is active. The heat flux boundary condition has a similar structure:

$$T = T_0 \quad on \quad \Gamma_D,$$
$$-\kappa \nabla T \cdot n = \begin{cases} q_{HF}\left(t, {}^{R}f, v_{CS}\right), & if \quad \vec{x} \in \Gamma_F(t), \\ 0, & otherwise. \end{cases} \tag{7}$$

The value v_{CS} denotes the cutting speed, i.e. the tangential velocity at the cutting edge. We estimate the heat flux into the work piece, q_{HF}, according to Müller [10]. The forces and torques acting on the cutter can be obtained by integrating equation (5) along the z-direction:

$$\begin{aligned} {}^{R}F &= \sum_{j=1}^{Nz} \int_{0}^{a_p} {}^{R}f(z_0 + \varsigma)\, d\varsigma, \\ {}^{C}M &= \sum_{j=1}^{Nz} \int_{0}^{a_p} g\left(\varphi_j(t, z_0 + \varsigma)\right) {}^{C}r\left(\alpha_j, z_0 + \varsigma\right) \times \left({}^{C}A_F\left(\alpha_j, z_0 + \varsigma\right)\hat{F}\right) d\varsigma. \end{aligned} \tag{8}$$

Note that we use the global reference frame to describe the force, while we describe the torque in the reference frame attached to the cutter. The vector ${}^{C}r\left(\alpha_j, z_0 + \varsigma\right)$ represents the distance between the center of mass of the cutter and the point on the cutting edge, where the respective cutting force is active. Finally, we project both values ${}^{R}F$ and ${}^{C}M$ on the space of generalized coordinates. Thus, we obtain a generalized force $G\left[{}^{R}F, {}^{C}M\right]$ contributing to the right hand side of equation (3) which is replaced by:

$$M(q,t)\ddot{q} = f(\dot{q}, q, t, p) + G\left[{}^{R}F, {}^{C}M\right]. \tag{9}$$

The crucial point is to derive an expression for the uncut chip thickness h. To this end, we look at a z=const plane and assume that cutter and work piece may oscillate independently.

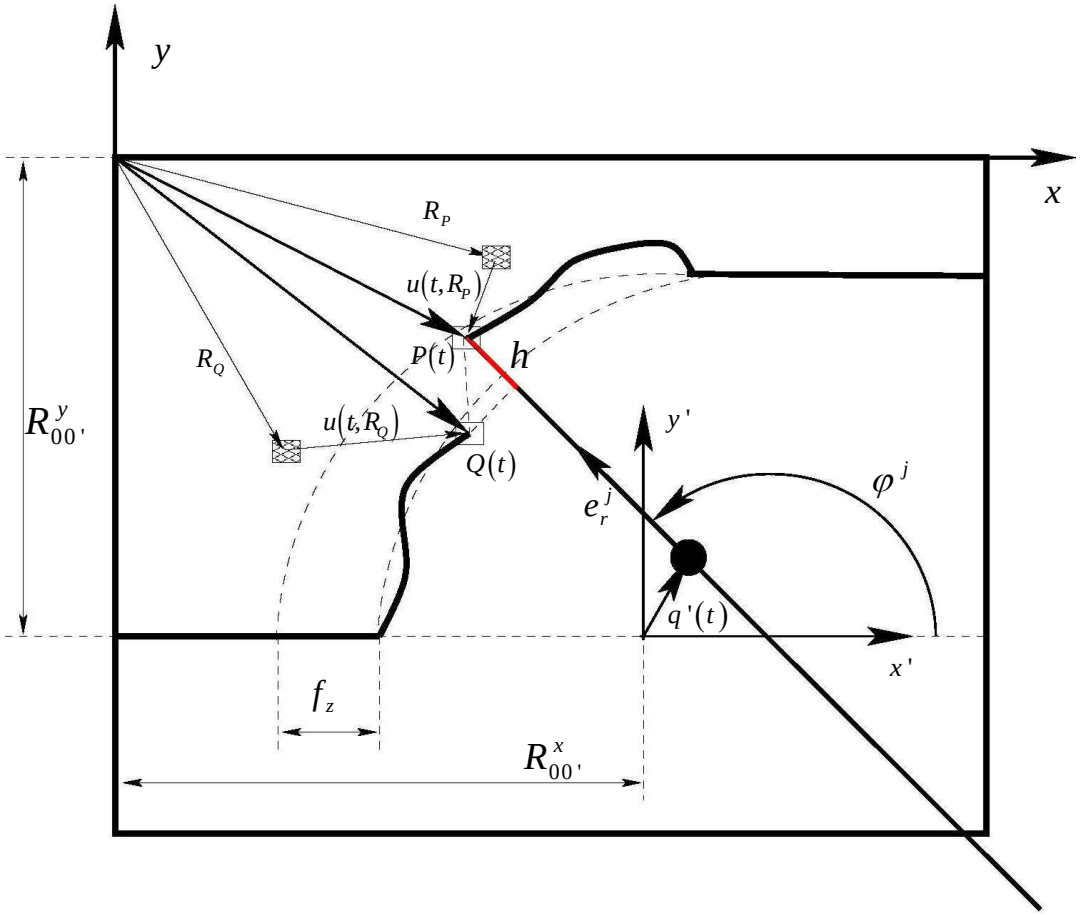

Figure 1: Scheme of the uncut chip thickness.

At a given time the cutter marks with its tip a certain material point R_P of the work piece moved to its position due to the deformation field $u(t,R_P)$. Thus, we may express the point $P(t)$ using on the one hand the work piece kinematics and on the other hand the cutter position:

$$\begin{aligned} P(t) &= u(t,R_P) + R_P, \\ &= R_{00'}(t) + \frac{D}{2} e_r^j + q'(t), \end{aligned} \tag{10}$$

where D denotes the diameter of the cutter. Usually, the uncut chip thickness is defined as:

$$h = \left(P(t) - Q(t)\right) \cdot e_r^j, \tag{11}$$

with e_r^j representing the unit vector in radial direction of tooth 'j' at time t. $Q(t)$ represents the relevant part of the work piece surface created during the preceding cut. Recall that at time $t-\tau$ the cutter marked another material point R_Q that was moved to its position due to the deformation field $u(t-\tau,R_Q)$. Thus equation (10) also holds at time $t-\tau$:

$$u(t-\tau,R_Q) + R_Q = R_{00'}(t-\tau) + \frac{D}{2} e_r^j + q'(t-\tau). \tag{12}$$

Furthermore, it is clear that the material point R_Q is also subject to the work piece deformation field $u(t,R_Q)$ at time t, which means that it is located at position $Q(t)$:

$$Q(t) = u(t,R_Q) + R_Q. \tag{13}$$

Finally, we may replace R_Q in equation (13) using equation (12), which yields the expression:

$$Q(t) = q'(t-\tau) + u\left(t, R_Q\right) - u\left(t-\tau, R_Q\right) + R_{00'}(t-\tau) + \frac{D}{2} e_r^j . \tag{14}$$

For the difference of $P(t)$ that we express with the second part of equation (10), and $Q(t)$ follows:

$$P(t) - Q(t) = R_{00'}(t) - R_{00'}(t-\tau) + q'(t) - q'(t-\tau) - \left(u\left(t, R_Q\right) - u\left(t-\tau, R_Q\right)\right). \tag{15}$$

We notice that the uncut chip thickness consists of three different parts. The first part represents just the cutter displacement due to the given feed. Projected on the radial direction, it yields the stationary uncut chip thickness. The second part represents the machine oscillations and produces the modulation of the chip thickness that has been indentified to be the main reason for chatter. The third contribution to the uncut chip thickness is related to the work piece deformation. While the first two terms are well-known, the third one is new. With this approach, for the first time, the influence of complex work piece dynamics on the stability of milling processes can be studied.

2.4 Numerical solution in time domain

In this subsection we briefly explain the numerical algorithm to solve the coupled system of equations (3) and (1) with (6) and (7). In a milling process with nonzero feed material is removed from the work piece. Since we use a thermo-elastic work piece representation that cannot take the chip removal into account directly, we have to introduce an approximation of this process. We therefore restrict ourselves to situations where only one tooth is in cut. Defining the theoretical tooth path by the positions of the cutting edge 'j' at time t and height z :

$$t_{th}^j(t,z) = R_{00'}(t) + \frac{D}{2} e_r^j\left(\varphi^j(t,z)\right), \tag{16}$$

neglecting all deformations, we estimate the shape of the machined work piece for the time interval $t \in \left[m\tau, (m+1)\tau\right]$ with $m \geq 0$. In equation (16) $\varphi^j(t,z)$ denotes the rotation angle of cutting edge « j » with respect to the z-slider for a rotation around the z-axis. When the active tooth leaves the cut, we create the newly shaped work piece and interpolate the solution from the old grid to the new one. Furthermore, we estimate R_Q appearing in equation (15) with the help of the theoretical tooth path:

$$\begin{aligned} u\left(t, R_Q\right) &\cong u\left(t, t_{th}^j(t,z)\right), \\ u\left(t-\tau, R_Q\right) &\cong u\left(t-\tau, t_{th}^j(t-\tau,z)\right). \end{aligned} \tag{17}$$

Thanks to these approximations we obtain a closed system of equations that we may solve numerically. The first step of the solution process is the transfer of the space-time continuous PDE system (cf. equation (1)) to a space discrete and time continuous set of equations. We therefore rewrite the balance equations in variational form and we use linear finite elements to derive the desired space discrete system. Afterwards we perform the time integration using an incremental decoupling. In order to sketch the algorithm, we start at time t^n assuming the solution $S^n \equiv \left(u_h^n, v_h^n, a_h^n, T_h^n, q^n\right)$ to be known, where $\dot{u}_h^n = v_h^n$ and $\dot{v}_h^n = a_h^n$. We compute the approximate solution S^{n+1} at time t^{n+1} carrying out the following steps:

- With S^n and the associated cutting forces, we calculate the update of the boundary conditions for the momentum and energy balance equation;
- We apply the Newmark algorithm (cf. Hughes [11]) to determine $u_h^{n+1}, v_h^{n+1}, a_h^{n+1}$ and a backward Euler scheme to solve the heat equation yielding, T_h^{n+1};

- Now we know $u_h^n, v_h^n, a_h^n, T_h^n$ and $u_h^{n+1}, v_h^{n+1}, a_h^{n+1}, T_h^{n+1}$. It is obvious that we may calculate each of these values at time $r \in \left[t^{n+1}, t^n \right]$ by means of interpolation. This also applies to every solution $S(s)$ with time $s \in \left[t^n - \tau, t^{n+1} - \tau \right]$. Thus, equation (9) reduces to a system of ordinary differential equations that we integrate with an explicit Runge-Kutta-54 solver (cf. Deufelhard et al. [12]). The outcome of this last step is the solution of the machine equation q^{n+1} and additionally the cutting forces at time t^{n+1}.
- Finally we store the calculated solution and restart the procedure.

After each tooth period the shape of the work piece is modified as explained above and then remeshed. Note that the whole algorithm has been implemented using the WIAS-pde-library pdelib2 [13]. It allows for direct access to all solution components guaranteeing efficient time stepping without any loss of performance due to data transfer.

3 PARAMETER IDENTIFCATION

We determine the cutting force coefficients using the method proposed by Altintas [14]. The main idea is to minimize a functional that compares measured average cutting forces with the outcome of the empirical cutting force model. Note that the method assumes stable cutting conditions. For further details we refer to Hömberg, et al. [15].

The heat flux into the work piece (cf. equation (7)) contains parameters, which have to be determined experimentally. We estimate the heat flux with the help of the cutting forces. The basic observation is that for dry cutting, the generated heat flows partly into the tool, partly into the chip and the work piece. With the help of an empirical parameter β_{CH} we extract the heat flowing into the work piece. The values for β_{CH} indicated in the pertinent literature range from 5-15%. However, in order to compute an acceptable estimate of the heat flux into the work piece, we have to determine β_{CH} more precisely. One possibility is to compare the simulated and the measured work piece temperature at several points close to the machined surface and to fit β_{CH} and the other parameters so that the difference between both temperatures be minimal.

The unknown machine parameters are the damping and stiffness constants appearing in the coupling elements. They are estimated on the basis of stiffness measurements.

4 NUMERICAL SIMULATIONS

We simulate a metal cutting process using the algorithm explained in Section 2.4. We consider a half immersion cut, with the cutter moving in negative x-direction (cf. Figure 1).

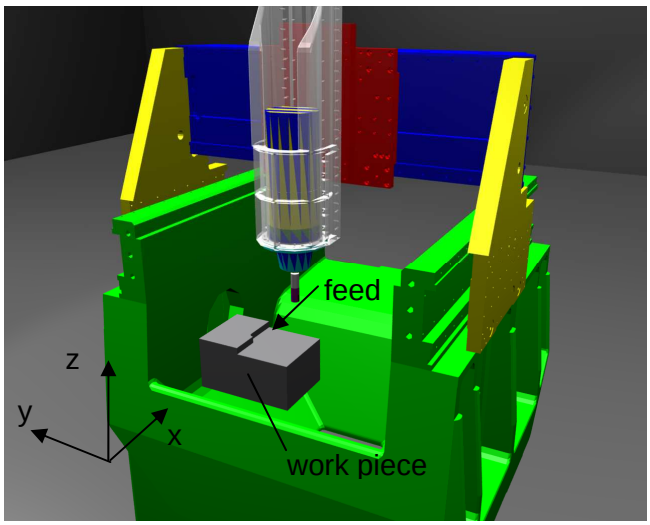

Figure 2: Machine model with work piece.

In order to illustrate what happens numerically if chatter occurs we compare a stable cut (axial depth of cut: $a_p = 0.75\,mm$) with an unstable solution (axial depth of cut: $a_p = 1.75\,mm$). We employ a 3 tooth helical end mill with a diameter of 15 mm and a helix angle of 10° as model for the cutter. The spindle speed was set 10000 rpm and we simulated 36 tooth periods of cutting.

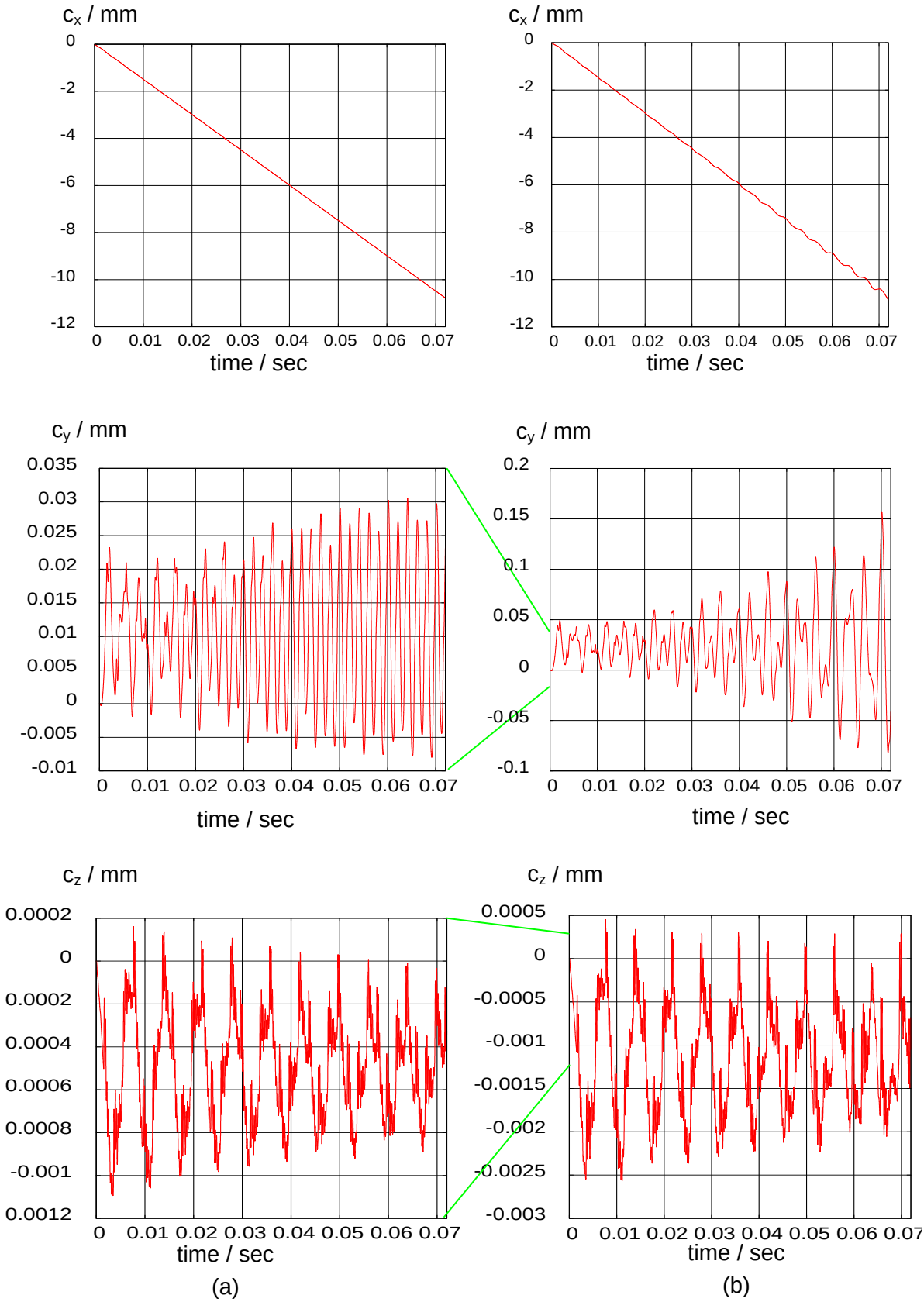

Figure 3: Displacement of the cutter tip (stable: (a), unstable (b)).

After a simulation run we evaluated the solution $q(t)$ at the tip of the cutter making use of equation (2). In the following we denote the vibrations at the tip of the cutter with $c(t) = {}^{R}h_{CT}(t, q(t)) - {}^{R}h_{CT}(t_0, q_0)$, where the index 'CT' represents the cutter tip. Figure 2 shows the x, y and z component of the cutter tip displacement. The pictures 3(a) depict the stable case while the pictures 3(b) show the unstable situation. The two diagrams in the first row clearly show the feed that is superposed with the cutter vibrations. For time $t > 0.05$ we recognize in picture (b) for c_x the increasing chatter vibrations. The y-component of the cutter tip displacement indicates the stable and the unstable cut. While the amplitude of c_y for the case (a) remains constant after the settling process, the amplitude of c_y in case (b) increases until the end of the simulation run, clearly indicating chatter. We prove this assessment with the help of the discrete fourier transform (DFT). Figure 4(b) shows a high chatter peak arising at about 290 Hz. The peaks and the harmonics related to the tooth

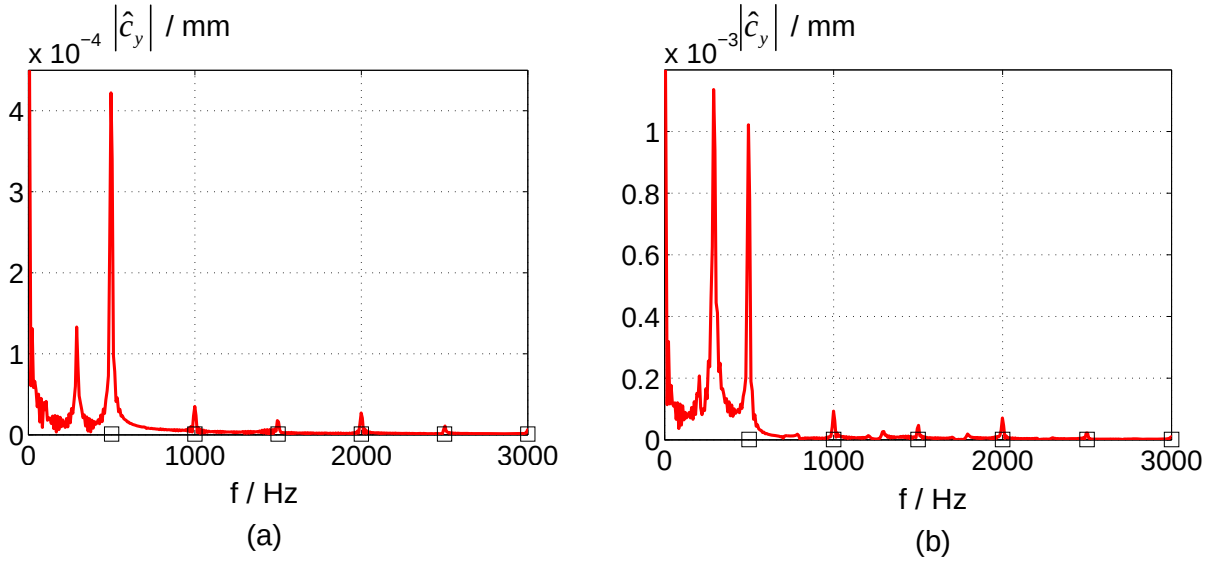

Figure 4: DFT of the y-component of the cutter displacement.

passing frequency arise at multiples of 500 Hz which are marked by the squares. In Figure 4 (b) the chatter peak dominates the peaks from the harmonic excitation which means that we are clearly in the regime of chatter. In Figure 4 (a) we also recognize a chatter peak, but this peak is clearly below the highest peak resulting from the excitation. We hence conclude that the cutting conditions corresponding to picture 4 (a) are much closer to the stability limit.

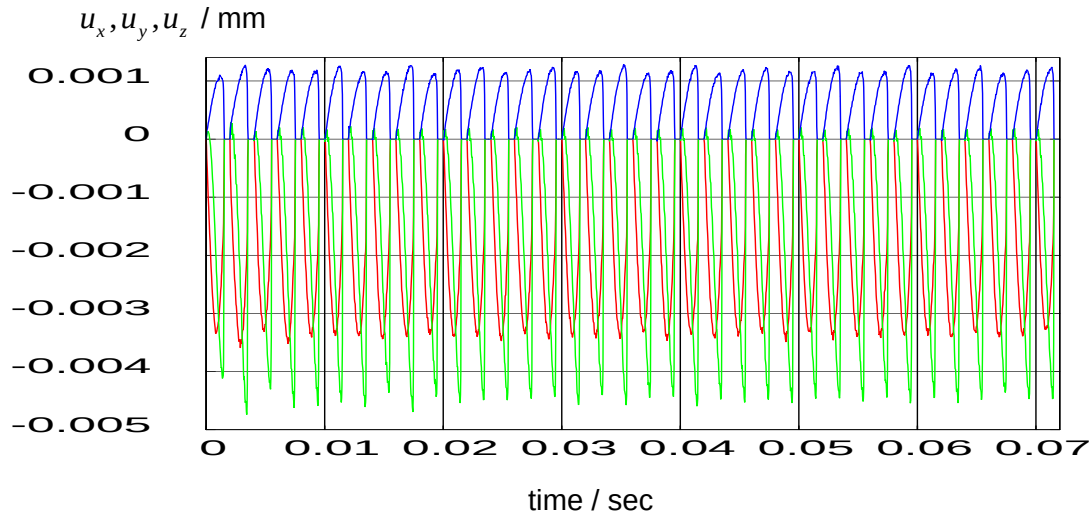

Figure 5: Work piece deformations in the stable case.

Finally we look at the work piece deformations. For the sake of simplicity we focus on the deformations occurring in the vicinity of the cutting edge at the top of the work piece. (cf. Figure 5 and 6). In both figures the red line denotes the deformation in x-direction, the green line the deformation in y-direction and the blue line the deformation in z-direction. Comparing both figures we state that in this case the work piece has no effect on the stability of the milling process. The amplitudes of the work piece deformations are much smaller than those of the cutter, which means that here the milling machine is the weakest part in the whole assembly. A second observation is that we eventually may distinguish stable and unstable processes also by analyzing the work piece deformations. Figure 6 indicates the unstable cut by increasing deformation amplitudes of the y-direction for $t > 0.05s$. Another hint for the unstable process is

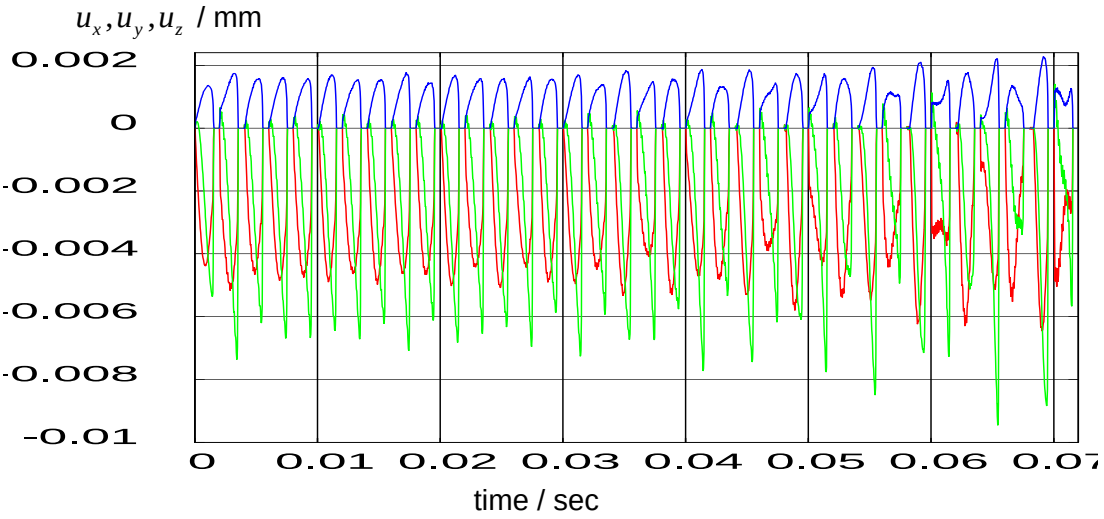

Figure 6: Work piece deformations in the unstable case.

the unstationary evolution of all deformation components for $t > 0.05s$.

5 CONCLUSION

In this paper we have developed an advanced milling model including several effects that can influence on the stability of milling processes. The main parts are a machine model represented by a multi body system and a work piece that is modeled as a thermo elastic solid. The coupling of both sub models was carried out with an empirical cutting force model that incorporates machine displacements and work piece deformation by a special model for the uncut chip thickness. Our main contribution is a new approach for the modeling of the uncut chip thickness that permits to account for the continuous work piece deformations. The system of coupled equations was solved with a time integration scheme taking care of the special features of the delayed ode-pde system. The presented simulations were carried out for realistic machine, work piece and cutting force parameters. However, the parameter identification including all necessary data for a precise thermal simulation is still in progress.

6 REFERENCES

[1] Altintas, Y., Weck, M., 2004, Chatter Stability of Metal Cutting and Grinding, Annals of the CIRP, 53/2, 619-642

[2] Faassen, R. P. H., Wouw, N. van de, Oosterling, J.A.J., Nijmeijer, H., 2003, Prediction of regenerative chatter by modeling and analysis of high-speed milling, International Journal of Machine Tools and Manufacture

[3] Faassen, R. P. H., 2007, Chatter Prediction and Control for High Speed Milling, Eindhoven University of Technology, ISBN 978-90-386-0995-9

[4] Insperger, T., Stépán, G., Upated semi-discretization method for periodic delay-differential equations with discrete delay, International Journal for Numerical Methods in Engineering

[5] Szalai, R., Stépán, G., 2006, Lobes and lenses in the stability chart of interrupted turning, ASME Journal of Computational and Nonlinear Dynamics, 205-211

[6] Haupt, P., 2000, Continuum mechanics and theory of materials, Advanced texts in physics, Springer, Berlin-Heidelberg-New York

[7] Pfeiffer, F., 1992, Einführung in die Dynamik, Leitfäden der Angewandten Mathematik und Mechanik LAMM, B. G. Teubner, Stuttgart

[8] Wittenburg, J., 1977, Dynamics of Systems of Rigid Bodies, Leitfäden der Angewandten Mathematik und Mechanik LAMM, B. G. Teubner, Stuttgart

[9] Weck, M., Teipel, K., 1977, Dynamisches Verhalten spanender Werkzeugmaschinen, Springer, Berlin-Heidelberg-New York

[10] Müller, B., 2004, Thermische Analyse des Zerspanens metallischer Werkstoffe bei hohen Schnittgeschwindigkeiten, Ph.D. thesis, Rheinisch-Westfälische Technische Hochschule Aachen

[11] Hughes, T.J.R, 2000, The Finite Element Method, Dover

[12] Deuflhard, P., Bornemann, F., 2002, Scientific Computing with Ordinary Differential Equations, Springer, Berlin-Heidelberg-New York

[13] pdelib2, http://www.wias-berlin.de/pdelib

[14] Altintas, Y., 2000, Manufacturing Automation, Cambridge University Press

[15] Hömberg, D., Mense, C., Rott, O., 2006, A comparison of analytical cutting force models, WIAS Preprint No. 1151